Communications in Theoretical Physics

Commun. Theor. Phys. **77** (2025) 105103 (11pp) https://doi.org/10.1088/1572-9494/adbbbc
CSTR: 32041.14.CTPadbbbc

EPR steering and Bell nonlocality via the filtering operation of two coupled double quantum dots system

Hao Wang

Shanghai Normal University Tianhua College, Shanghai 201815, China

E-mail: shnuwh@163.com

Received 23 October 2024, revised 26 December 2024
Accepted for publication 25 February 2025
Published 13 June 2025

Abstract

In this work, we mainly study Bell nonlocality and quantum steerability of two-coupled double quantum dots (DQDs) system via local filtering operation. We compare and analyze the influence of the Coulomb potential, temperature, tunneling parameter and local filtering operation on quantum steering and Bell nonlocality in the system. The results show that quantum steering and nonlocality first increase and then decrease but never vanish even for the stronger value of the Coulomb potential. Quantum steering and Bell nonlocality would degrade with the increase of temperature. The filtering process does not increase the degree of steerability, but decreases the range of quantum steerability. In addition, it is noteworthy that a peculiar phenomenon exists: the Einstein–Podolsky–Rosen (EPR) steering asymmetry between Alice and Bob first increase, then decrease to zero and finally increases as the tunneling strength increases. However, this phenomenon does not appear with no operation between Alice and Bob.

Keywords: double quantum dots, EPR steering, Bell nonlocality, quantum steerability, filtering operation

(Some figures may appear in colour only in the online journal)

1. Introduction

Quantum correlations, including quantum discord [1], quantum entanglement [2], quantum steering [3] and Bell nonlocality (BN) [4], are indispensable in quantum communication and quantum computation, which are impossible tasks for classical correlations. Quantum discord is an information-theoretic measure of nonclassical correlations that goes beyond entanglement, introduced by Ollivier and Zurek [5], which is defined as the difference between the total correlation and the classical correlation. Quantum entanglement is an intermediate type of quantum correlation between quantum steering and discord. It has been viewed as an important resource for quantum key distribution, quantum cryptograph and quantum teleportation [6]. The Einstein–Podolsky–Rosen (EPR) steering, first proposed by Schrödinger to verify the EPR paradox, is a form of bipartite quantum correlation, intermediate to the concepts of entanglement and Bell nonlocality. Quantum steering has stimulated an important concept of 'quantum nonlocality,' which manifests itself in three types: quantum entanglement, quantum steering, and Bell's nonlocality. Entanglement, EPR steering and Bell's nonlocality have an interesting hierarchical structure: quantum entanglement is a superset of steering, and Bell's nonlocality is a subset of steering [7]. Although Bell's nonlocality is more often used to show 'quantum nonlocality,' the original EPR paradox is essentially a steering paradox. Quantum nonlocality is an essential characteristic of quantum physics, which is dramatically different from classical physics and has been considered to be the foundation of quantum information and quantum computation.

EPR steering describes the ability of one observer to affect the state of another remote observer via local measurements. In 2007, Wiseman *et al* [8] strictly redefined quantum steering. Subsequently, Walborn *et al* [9, 10]. used the entropy uncertainty relationship (EUR) to derive the EPR steering inequality. In 2014, Skrzypczyk *et al* [11] proposed

the quantity steerable weight (SW) to describe the ability of quantum steering. Suppose Alice and Bob share a pair of two-qubit state, it is not hard to imagine that if Alice entangles with Bob, then Bob must also entangle with Alice. Such a symmetric feature holds for both entanglement and Bell nonlocality. In fact, in the case of entanglement and Bell nonlocality, Alice and Bob can be freely interchanged. However, in EPR steering, Alice's ability to steer Bob's state may not be equal to Bob's ability to steer Alice's state. This formal asymmetry can never be found in entanglement or Bell nonlocality. EPR steering is a significant quantum phenomenon in which a quantum state can be non-locally changed or steered to another state remotely by performing some local measurements. There are situations where Alice can steer Bob's state but Bob cannot steer Alice's state, or vice versa, which are referred to as one-way EPR steering [12]. Recently, quantum steering has attracted increasing attention for both theoretical and experimental investigations [13–15] because of the potential applications in quantum information processing, such as the quantum key distribution [16], asymmetric quantum network [17], randomness generation [18, 19] and randomness certification [20].

In 1964, based on the Einstein's local realism, Bell derived the famous Bell inequality for local hidden variable (LHV) models [4]. Bell inequalities offer a way to contrast predictions of certain hidden variable theories with experimental observations [21]. In addition, Bell's inequalities appear to be equivalent to the Clauser–Horner–Shimony–Holt (CHSH) inequality [22]. The CHSH inequality has been mostly used for detecting and quantifying the Bell nonlocality of two qubits [23], which has been experimentally tested [24, 25]. The violation of Bell's inequality by quantum entangled states implies Bell's nonlocality whose correlations cannot be explained in terms of any LHV model. Bell nonlocality refers to correlations between two distant, entangled particles that challenge classical notions of local causality. Beyond its foundational significance, nonlocality is crucial for device-independent technologies like quantum key distribution and randomness generation [26, 27]. In general, Bell nonlocality can detect by either the Bell inequality or the CHSH inequality, which indicates that the quantum world has the characteristics of non-localization. The violation of Bell inequality (especially the Bell-CHSH inequality [22]) provides an unambiguously measurement of Bell nonlocality, which has been proved both theoretically and experimentally [28, 29]. In terms of the Bell nonlocality concept [30, 31], the nonlocal character of a quantum state lies in the violation of the Bell inequalities. Such a nonclassical feature of quantum mechanics can be used in device-independent quantum information processing [32]. Nonlocality quickly deteriorates in the presence of noise, and restoring nonlocal correlations requires additional resources. As a sort of stronger quantum correlation, Bell nonlocality is an important quantum resource in the course of quantum computation and quantum communication and cannot be reproduced by any classical local model.

Studying theoretical quantum information quantifiers in condensed matter physics systems is crucial for various information processing protocols. One of the most promising physical systems for implementing quantum technologies, particularly quantum computing, is solid-state quantum dots (QDs). Quantum dots and double quantum dots are promising options for quantum information processing, utilizing Coulomb interaction and tunneling effects to create stable and controllable quantum states. These solid-state-based systems offer scalability and tools available for information control, retrieval, and inscription. The characterization of quantum correlations in coupled double quantum dots has gained increasing interest among researchers [33–38].

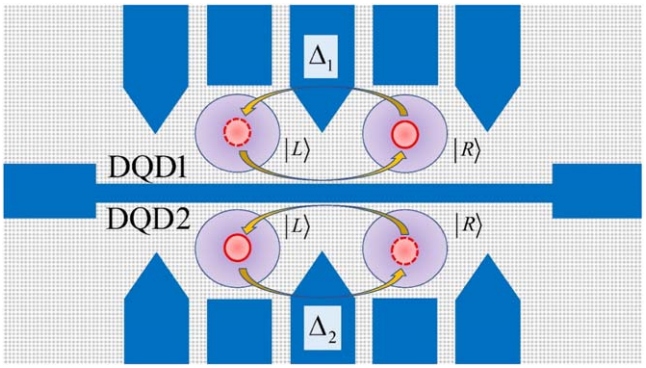

Figure 1. Schematic diagram of the physical model of the two-coupled DQDs with two excess electrons localized at the left (right) side of the top (bottom) DQD.

In this paper, we study the nonlocal properties, EPR steering and Bell nonlocality in the model of two-coupled double quantum dots (DQDs) and propose a scheme to improve the quantum steering and nonlocality by local filtering operation. The paper is organized as follows. In section 2, we briefly introduce the model of the two-coupled DQDs system. In section 3, we give review some basic definitions about quantum steering (or EPR steering) and Bell nonlocality and elaborate the behavior of the steering and nonlocality under the different parameters. In section 4, we improve the ability of steering and nonlocality via local filtering operation. Finally, we provide a brief conclusion in section 5.

2. Physical model and thermal density matrix

The physical model consists of the two-coupled DQDs system (see figure 1), in which each of the two excess electrons have two degrees of freedom and can be found either in the left quantum dot $|L\rangle$ or in the right one $|R\rangle$. The Hamiltonian of such a system is given by [39–41]

$$\hat{H} = \sum_{i=1}^{2} \Delta_i \sigma_x^i + V(\sigma_z^1 \otimes \sigma_z^2), \tag{1}$$

where $\Delta_1(\Delta_2)$ is the energy of the tunneling coupling between each pair of quantum dots and V represents the strength of the Coulomb interaction between two excess electrons. $\sigma_{x,y,z}^{1(2)}$ are the Pauli matrices, where $\sigma_x = |L\rangle\langle R| + |R\rangle\langle L|$ and $\sigma_z = |L\rangle\langle L| - |R\rangle\langle R|$. In the standard computing basis of

$\{|LL\rangle, |LR\rangle, |RL\rangle, |RR\rangle\}$, the matrix form of the Hamiltonian then reads

$$\hat{H} = \begin{pmatrix} V & \Delta_2 & \Delta_1 & 0 \\ \Delta_2 & -V & 0 & \Delta_1 \\ \Delta_1 & 0 & -V & \Delta_2 \\ 0 & \Delta_1 & \Delta_2 & V \end{pmatrix}. \tag{2}$$

The eigenvalues are evaluated as

$$\begin{aligned} E_1 &= \sqrt{V^2 + (\Delta_1 - \Delta_2)^2}, \\ E_2 &= -\sqrt{V^2 + (\Delta_1 - \Delta_2)^2}, \\ E_3 &= \sqrt{V^2 + (\Delta_1 + \Delta_2)^2}, \\ E_4 &= -\sqrt{V^2 + (\Delta_1 + \Delta_2)^2}, \end{aligned} \tag{3}$$

and the corresponding eigenvectors are given by

$$\begin{aligned} |\psi_1\rangle &= A_+[a_+(-|LL\rangle + |RR\rangle) + (-|LR\rangle + |RL\rangle)], \\ |\psi_2\rangle &= A_-[a_-(-|LL\rangle + |RR\rangle) + (-|LR\rangle + |RL\rangle)], \\ |\psi_3\rangle &= B_+[b_+(|LL\rangle + |RR\rangle) - (|LR\rangle + |RL\rangle)], \\ |\psi_4\rangle &= B_-[b_-(|LL\rangle + |RR\rangle) - (|LR\rangle + |RL\rangle)], \end{aligned} \tag{4}$$

where $A_\pm = \frac{1}{\sqrt{2}\sqrt{a_\pm^2+1}}$, $B_\pm = \frac{1}{\sqrt{2}\sqrt{b_\pm^2+1}}$, $a_\pm = \frac{V \pm \sqrt{V^2+\Delta_-^2}}{\Delta_-}$, $b_\pm = \frac{V \pm \sqrt{V^2+\Delta_+^2}}{\Delta_+}$ and $\Delta_\pm = \Delta_1 \pm \Delta_2$.

The state of the two-coupled DQDs system in the thermal equilibrium is described by

$$\hat{\varrho}(T) = \frac{1}{Z} e^{-\hat{H}/k_B T}, \tag{5}$$

in which the partition function is $Z = \mathrm{Tr}(e^{-\hat{H}/k_B T})$, k_B is the Boltzmann's constant and T is the temperature. The thermal density matrix $\hat{\varrho}(T)$ can be analytically derived by using the spectral decomposition of the Hamiltonian. The density matrix of the system in the standard basis $\{|LL\rangle, |LR\rangle, |RL\rangle, |RR\rangle\}$ takes the following form

$$\hat{\varrho}(T) = \begin{pmatrix} \hat{\varrho}_{11} & \hat{\varrho}_{12} & \hat{\varrho}_{13} & \hat{\varrho}_{14} \\ \hat{\varrho}_{12} & \hat{\varrho}_{22} & \hat{\varrho}_{23} & \hat{\varrho}_{13} \\ \hat{\varrho}_{13} & \hat{\varrho}_{23} & \hat{\varrho}_{22} & \hat{\varrho}_{12} \\ \hat{\varrho}_{14} & \hat{\varrho}_{13} & \hat{\varrho}_{12} & \hat{\varrho}_{11} \end{pmatrix}, \tag{6}$$

where, the corresponding entries are provided by

$$\begin{aligned} \varrho_{11} &= \frac{1}{4Z}[\Gamma_+ e^{-\beta e_1} + \Gamma_- e^{-\beta e_2} + \Lambda_+ e^{-\beta e_3} + \Lambda_- e^{-\beta e_4}], \\ \varrho_{12} &= \frac{1}{4Z}[\Omega_-(-e^{-\beta e_1} + e^{-\beta e_2}) + \Omega_+(e^{-\beta e_3} - e^{-\beta e_4})], \\ \varrho_{13} &= \frac{1}{4Z}[\Omega_-(e^{-\beta e_1} - e^{-\beta e_2}) + \Omega_+(e^{-\beta e_3} - e^{-\beta e_4})], \\ \varrho_{14} &= \frac{1}{4Z}[-\Gamma_+ e^{-\beta e_1} - \Gamma_- e^{-\beta e_2} + \Lambda_+ e^{-\beta e_3} + \Lambda_- e^{-\beta e_4}], \\ \varrho_{22} &= \frac{1}{4Z}[\Gamma_+ e^{-\beta e_1} + \Gamma_- e^{-\beta e_2} + \Lambda_+ e^{-\beta e_3} + \Lambda_- e^{-\beta e_4}], \\ \varrho_{23} &= \frac{1}{4Z}[-\Gamma_- e^{-\beta e_1} - \Gamma_+ e^{-\beta e_2} + \Lambda_- e^{-\beta e_3} + \Lambda_+ e^{-\beta e_4}], \end{aligned} \tag{7}$$

where $\Lambda_\pm = 1 \pm \frac{V}{\sqrt{V^2+\Delta_+^2}}$, $\Gamma_\pm = 1 \pm \frac{V}{\sqrt{V^2+\Delta_-^2}}$ and $\Omega_\pm = \frac{\Delta_\pm}{\sqrt{V^2+\Delta_\pm^2}}$. The partition function of the system is given by $Z = 2[\cosh(\beta\sqrt{V^2+\Delta_+^2}) + \cosh(\beta\sqrt{V^2+\Delta_-^2})]$. The centrosymmetric matrix $n \times n$ is defined by the relations for its matrix elements as follows: $a_{ij} = a_{n+1-i,n+1-j}$ [42]. The state (6) has the centrosymmetric (CS) matrix. The thermal density matrix $\hat{\varrho}(T)$ equation (6), as previously mentioned, will be used to quantify the quantum correlations that exist between two-coupled double quantum dots through the EPR steering and Bell nonlocality quantifiers.

3. Measures of quantum correlations

In this section, we give a brief review concerning the definition and properties of the EPR steering and Bell nonlocality. We elaborate the steering and nonlocality under the difference parameters.

3.1. Entropic steering

Considering discrete observables $\hat{R}$ and $\hat{S}$ with outcomes$\{|R_i\rangle\}$ and $\{|S_j\rangle\}$, respectively, and where i runs from 1 to the total number of distinct eigenstates N, there exists the entropic uncertainty relation

$$\mathcal{H}_Q(R) + \mathcal{H}_Q(S) \geqslant \log_2 U, \tag{8}$$

where $U = \min_{i,j} \frac{1}{|\langle R_i \mid S_j\rangle|^2}$. Using the discrete entropic uncertainty relation equation (8), along with local hidden state (LHS) constraint for discrete observables

$$\mathcal{H}(R^B|R^A) \geqslant \sum_\lambda P(\lambda)\mathcal{H}_Q(R^B|\lambda), \tag{9}$$

where $\mathcal{H}_Q(R^B|\lambda)$ is the discrete Shannon entropy of the probability distribution $P_Q(R^B|\lambda)$, where the subscript Q means that it corresponds to a quantum state. We immediately arrive at an entropic steering inequality for pairs of discrete observables,

$$\mathcal{H}(R^B|R^A) + \mathcal{H}(S^B|S^A) \geqslant \log_2(U^B), \tag{10}$$

where U^B denotes the value of U associated with observables R^B and S^B. This steering inequality that involves a pair of discrete observables may be generalized to the more general case that involves arbitrary number of mutually unbiased observables. In two-dimensional quantum systems, employing the Pauli measurements base on each side, and the entropy uncertainty relation (EUR) steering inequality reads [43].

$$\mathcal{I}_{ab} = \hat{\mathcal{H}}(\hat{\sigma}_x^{(b)}|\hat{\sigma}_x^{(a)}) + \hat{\mathcal{H}}(\hat{\sigma}_y^{(b)}|\hat{\sigma}_y^{(a)}) + \hat{\mathcal{H}}(\hat{\sigma}_z^{(b)}|\hat{\sigma}_z^{(a)}) \geqslant 2, \tag{11}$$

where $(\hat{\sigma}_x, \hat{\sigma}_y, \hat{\sigma}_z)$ represent the Pauli spin operator as measurements and the symbol $\mathcal{H}$ stands for the Shannon entropy and $\mathcal{H}(R_b|R_a) = \mathcal{H}(\hat{\varrho}_{ab}) - \mathcal{H}(\hat{\varrho}_a)$ represents the conditional Shannon entropy. Quantum steering is demonstrated when the inequality is violated. By using Pauli matrices $\hat{\sigma} = (\hat{\sigma}_x, \hat{\sigma}_y, \hat{\sigma}_z)$ measurements, one can simplify the expression of EPR

steering inequality in equation (11) reads,

$$\mathcal{I}_{ab} = \frac{1}{2}\sum_{i=1}^{4}\begin{bmatrix}(P_{x_i}^{ab})\log_2(P_{x_i}^{ab})\\ +(P_{y_i}^{ab})\log_2(P_{y_i}^{ab})\\ +(P_{z_i}^{ab})\log_2(P_{z_i}^{ab})\end{bmatrix} - \sum_{i=1}^{2}\begin{bmatrix}(P_{x_i}^{a})\log_2(P_{x_i}^{a})\\ +(P_{y_i}^{a})\log_2(P_{y_i}^{a})\\ +(P_{z_i}^{a})\log_2(P_{z_i}^{a})\end{bmatrix}, \tag{12}$$

where $P_{x_i}^{ab}$, $P_{y_i}^{ab}$ and $P_{z_i}^{ab}$ represent the eigenvalues of the density operator $\hat{\varrho}(T)$. Explicitly, they are given by

$$\begin{aligned}
P_{x_1}^{ab} &= 1 + 2(\hat{\varrho}_{13} + 2\hat{\varrho}_{14} + \hat{\varrho}_{24}),\\
P_{x_2}^{ab} &= 1 - 2(\hat{\varrho}_{13} - 2\hat{\varrho}_{14} + \hat{\varrho}_{24}),\\
P_{x_3}^{ab} &= 1 - 2(-\hat{\varrho}_{13} + 2\hat{\varrho}_{14} - \hat{\varrho}_{24}),\\
P_{x_4}^{ab} &= 1 + 2(-\hat{\varrho}_{13} - 2\hat{\varrho}_{14} - \hat{\varrho}_{24}),\\
P_{y_1,y_2,y_3,y_4}^{ab} &= 1,\\
P_{z_i}^{ab} &= 4\hat{\varrho}_{ii}.
\end{aligned} \tag{13}$$

Likewise, $P_{x_i}^{a}$, $P_{y_i}^{a}$ and $P_{z_i}^{a}$ are the eigenvalues of the reduced density operator $\hat{\varrho}_A$, where,

$$P_{x_1,x_2}^{a} = 1 \pm 2(\hat{\varrho}_{13} + \hat{\varrho}_{24}),\ P_{y_1,y_2}^{a} = P_{z_1,z_2}^{a} = 1. \tag{14}$$

The degree of steerability is quantified based on Alice's measurements as follows [44, 45]

$$\mathcal{S}_{A\to B} = \max\left\{0, \frac{\mathcal{I}_{ab} - 2}{\mathcal{I}_{\max} - 2}\right\}, \tag{15}$$

where $\mathcal{I}_{\max} = 6$ is calculated for a system initially prepared in Bell states. The factor $(\mathcal{I}_{\max} - 2)$ is introduced to ensure that the steering process is normalized. By exchanging the roles of A and B, the possibility of the steering by performing measurements on the subsystem B is given by,

$$\mathcal{S}_{B\to A} = \max\left\{0, \frac{\mathcal{I}_{ba} - 2}{\mathcal{I}_{\max} - 2}\right\}, \tag{16}$$

where $\mathcal{I}_{ba}$ quantifies the steering from Bob to Alice, it is given by,

$$\mathcal{I}_{ba} = \frac{1}{2}\sum_{i=1}^{4}\begin{bmatrix}(P_{x_i}^{ab})\log_2(P_{x_i}^{ab})\\ +(P_{y_i}^{ab})\log_2(P_{y_i}^{ab})\\ +(P_{z_i}^{ab})\log_2(P_{z_i}^{ab})\end{bmatrix} - \sum_{i=1}^{2}\begin{bmatrix}(P_{x_i}^{b})\log_2(P_{x_i}^{b})\\ +(P_{y_i}^{b})\log_2(P_{y_i}^{b})\\ +(P_{z_i}^{b})\log_2(P_{z_i}^{b})\end{bmatrix}, \tag{17}$$

with,

$$P_{x_1,x_2}^{b} = 1 \pm 2(\hat{\varrho}_{11} - \hat{\varrho}_{22}),\ P_{y_1,y_2}^{b} = P_{z_1,z_2}^{b} = 1. \tag{18}$$

Unlike quantum entanglement and Bell nonlocality, quantum steering may not be symmetrical, i.e. $\mathcal{S}_{A\to B} = \mathcal{S}_{B\to A}$. EPR steering exhibits distinct asymmetric characteristics and serves as the necessary quantum resource for one-sided device-independent quantum information tasks. The difference between $\mathcal{S}_{A\to B}$ and $\mathcal{S}_{B\to A}$ is introduced by

$$\mathcal{S}_{\Delta_{AB}} = |\mathcal{S}_{B\to A} - \mathcal{S}_{A\to B}|, \tag{19}$$

which represents the degree of asymmetry between $\mathcal{S}_{A\to B}$ and $\mathcal{S}_{B\to A}$ in different orientations.

3.2. Bell-CHSH inequality

Using the Bloch representation, an arbitrary two-qubit state can be expressed as

$$\hat{\varrho} = \frac{1}{4}\left(\hat{I}\otimes\hat{I} + \hat{\boldsymbol{r}}\cdot\hat{\sigma}\otimes\hat{I} + \hat{I}\otimes\hat{\boldsymbol{s}}\cdot\hat{\sigma} + \sum_{i,j=1}^{3}\mathcal{T}_{ij}\hat{\sigma}_i\otimes\hat{\sigma}_j\right), \tag{20}$$

where $\hat{I}$ is 2×2 identity matrix, $r_i = \mathrm{Tr}[\hat{\varrho}(\hat{\sigma}_i\otimes\hat{I})]$ and $s_i = \mathrm{Tr}[\hat{\varrho}(\hat{I}\otimes\hat{\sigma}_i)]$ are Bloch vectors of Alice's and Bob's qubit, respectively, $\mathcal{T}_{ij} = \mathrm{Tr}[\hat{\varrho}(\hat{\sigma}_i\otimes\hat{\sigma}_j)]$ are correlation matrix elements. $\hat{\sigma} = (\hat{\sigma}_x, \hat{\sigma}_y, \hat{\sigma}_z)$ is a vector of the Pauli matrices, with $\hat{\sigma}_x = |0\rangle\langle 1| + |1\rangle\langle 0|$, $\hat{\sigma}_y = i(|0\rangle\langle 1| - |1\rangle\langle 0|)$ and $\hat{\sigma}_z = |0\rangle\langle 0| - |1\rangle\langle 1|$. here $\boldsymbol{r} = (r_x, r_y, r_z)$, $\boldsymbol{s} = (s_x, s_y, s_z)$, with $|\boldsymbol{r}| \leqslant 1, |\boldsymbol{s}| \leqslant 1$ and $(\mathcal{T}_{ij})$ is the correlation matrix.

The Bell-CHSH inequality quantifies the correlations arising from local measurements on two-qubit states. All correlations which violate the inequality are termed as nonlocal as they defy explanation by any local hidden variable model (LHVM). The Bell-CHSH inequality for the mixed state equation (6) can be written as [6, 46]

$$\langle\!\langle\mathcal{B}_{\mathrm{CHSH}}\rangle\!\rangle = |\mathrm{Tr}(\hat{\varrho}\mathcal{B}_{\mathrm{CHSH}})| \leqslant 2 \tag{21}$$

in terms of the Bell-CHSH operator

$$\mathcal{B}_{\mathrm{CHSH}} = \boldsymbol{a}\cdot\hat{\sigma}\otimes(\boldsymbol{b} + \boldsymbol{b}')\cdot\hat{\sigma} + \boldsymbol{a}'\cdot\hat{\sigma}\otimes(\boldsymbol{b} - \boldsymbol{b}')\cdot\hat{\sigma}, \tag{22}$$

where $\boldsymbol{a}, \boldsymbol{a}', \boldsymbol{b}$ and $\boldsymbol{b}'$ are unit vectors in three-dimensional describing the measurements on sides Alice and Bob, respectively. Based on the Horodecki theorem [6, 46], the maximum expected value of the Bell-CHSH operator for the given state $\hat{\varrho}$ is given by

$$\mathcal{B}_{\mathrm{Bell-CHSH}} = \max_{\mathcal{B}_{\mathrm{CHSH}}} Tr(\hat{\varrho}\mathcal{B}_{\mathrm{CHSH}}) = 2\sqrt{\max_{i<j}(\mu_i + \mu_j)}, \tag{23}$$

where $\mu_i (i = 1, 2, 3)$ are the eigenvalues of the real symmetric matrix $\hat{\mathcal{U}} = \hat{\mathcal{T}}^t\hat{\mathcal{T}}$ constructed from the correlation matrix $\hat{\mathcal{T}}$ and its transpose $\hat{\mathcal{T}}^t$ For the mixed state equation (6), we can obtain the Bell-CHSH inequality

maximum violation by the following form

$$\begin{aligned}\mathcal{B}_{\text{Bell}-\text{CHSH}} &= 2\max\{\mathcal{B}_1, \mathcal{B}_2, \mathcal{B}_3\},\\ \mathcal{B}_1 &= \sqrt{\mu_1+\mu_2},\\ \mathcal{B}_2 &= \sqrt{\mu_1+\mu_3},\\ \mathcal{B}_3 &= \sqrt{\mu_2+\mu_3},\end{aligned} \tag{24}$$

where

$$\begin{aligned}\mu_1 &= -16\varrho_{12}^2,\\ \mu_2 &= -16\varrho_{14}^2,\\ \mu_3 &= 4(\varrho_{13}-\varrho_{24})^2.\end{aligned} \tag{25}$$

Finally, the normalized form of Bell nonlocality quantifier can be written as [23, 47, 48]

$$\mathcal{B}(\hat{\varrho}) = \max\left\{0, \frac{\mathcal{B}_{\text{Bell}-\text{CHSH}}(\hat{\varrho})-2}{\mathcal{B}_{\max}(\hat{\varrho})-2}\right\}, \tag{26}$$

where $0 \leqslant \mathcal{B}(\hat{\varrho}) \leqslant 1$ since $\mathcal{B}_{\text{Bell}-\text{CHSH}}(\hat{\varrho}) \leqslant \mathcal{B}_{\max}(\hat{\varrho}) \leqslant 2\sqrt{2}$ for a bipartite system.

The Bell nonlocality $\mathcal{B}(\hat{\varrho})$, quantum steerability $\mathcal{S}_{A\to B}(\hat{\varrho})$ and $\mathcal{S}_{B\to A}(\hat{\varrho})$ of the state in equation (7) are plotted against the Coulomb potential V, tunneling parameter Δ_1 and temperature T in figure 2. It is observed that the behavior of the Bell nonlocality and quantum steerability is similar in the two-coupled DQDs system. As described in figures 2(a) and (b), the increase of the Coulomb potential V cannot affect Bell nonlocality and quantum steerability in the initial stage. These quantum nonlocalities are frozen at different fixed values, respectively. However, the variations of Bell nonlocality and quantum steerability show a very rapid increase for the small values of the Coulomb potential V and tunneling parameter Δ_1, from zero to maximum values and then decrease with the increase of the Coulomb potential V or tunneling parameter Δ_1. Moreover, we note that the quantum steerability cannot surpass the Bell nonlocality.

Figure 2(a) shows that Bell nonlocality and quantum steerability is absent when the Coulomb potential is zero for several values of $T = 1.0$, $\Delta_1 = 10\,\mu\text{eV}$ and $\Delta_2 = 3\,\mu\text{eV}$. This result shows that the Coulomb potential can be used for either turning on or off the quantum steering and Bell nonlocality. We note that the amounts of the Bell nonlocality and quantum steerability display an increasing behavior until a threshold value of the Coulomb potential V_C and then decrease, but never vanish even for stronger values of the interaction coupling parameters. It becomes clear that the Coulomb interaction between the two excess electrons have to be adjusted to a specific interval to utilize quantum steering and Bell nonlocality for better resourcefulness in the two-coupled DQDs state.

To further understand the modulation of the Bell nonlocality and quantum steerability, we plot the Bell nonlocality and quantum steerability as functions of the tunneling parameter Δ_1, as shown in figure 2(b). We can observe that Bell nonlocality and quantum steerability vanishes when tunneling parameter $\Delta_1 = 0$ regardless of the values of tunneling parameter Δ_2. In this case, the two-coupled DQDs system are not entangled, because the electron can no longer move

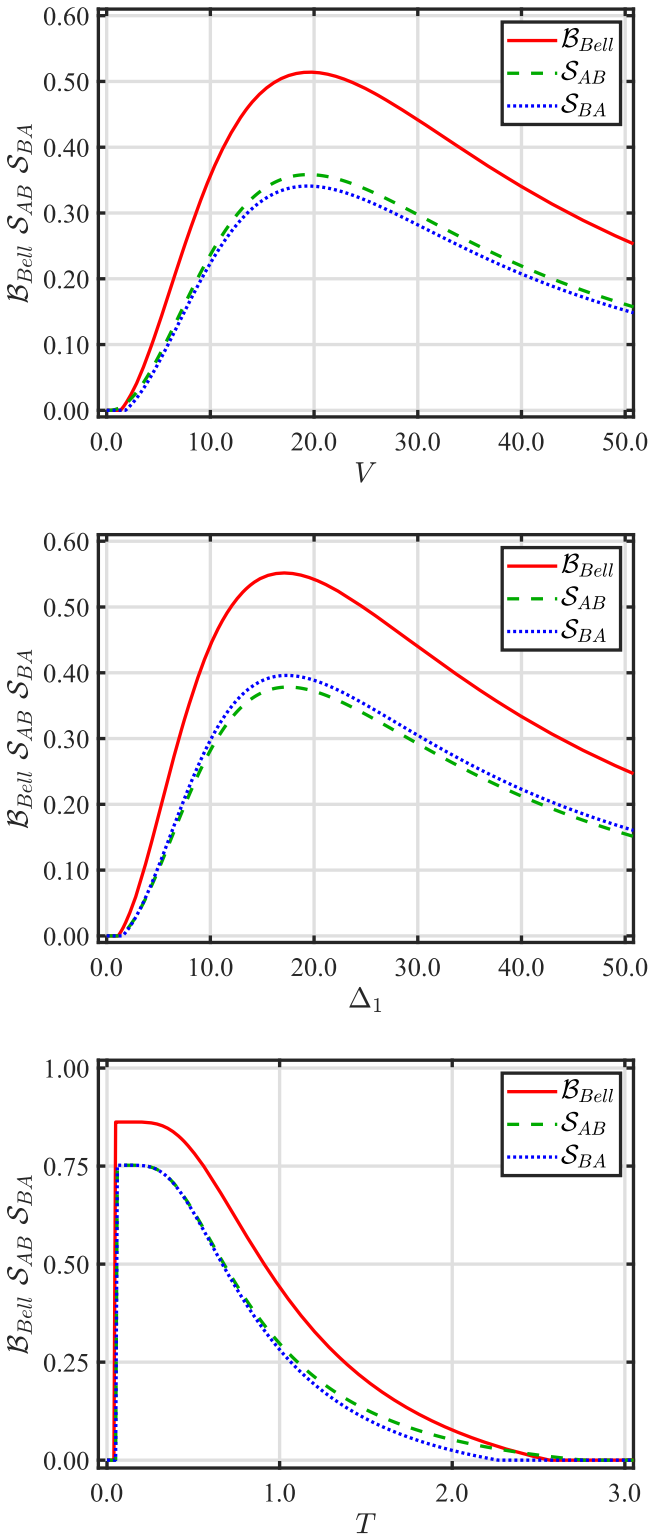

Figure 2. Bell nonlocality and quantum steerability as a function of various parameters. (a) Coulomb potential V with $T = 1.0$, $\Delta_1 = 10\,\mu eV$ and $\Delta_2 = 3\,\mu eV$ (b) the tunneling parameters Δ_1 with $T = 1.0$, $V = 20\,\mu eV$ and $\Delta_2 = 3\,\mu eV$ (c) temperature T with $V = 20\,\mu eV$, $\Delta_1 = 10\,\mu eV$ and $\Delta_2 = 3\,\mu eV$. The fixed parameter is $k_B = 1$.

within the double quantum dots. It can be seen from figure 2(b), that the Bell nonlocality and quantum steerability first increase and then decrease as tunneling strength Δ_1 increases. It should be stressed that Bell nonlocality is much

greater than quantum steerability in general, but the quantum steering $\mathcal{S}_{A\to B}$ may be larger or smaller than quantum steering $\mathcal{S}_{B\to A}$ for weaker values of the tunneling strength parameters. Moreover, it is worth noting that the perfect transfer of the asymmetric quantum EPR steering can also be realized in such a two-coupled DQDs system.

In order to investigate the influences of temperature on quantum steering, and Bell nonlocality, we characterize the dependence of quantum steering, and Bell nonlocality on the temperature. Figure 2(c) shows that both quantum steering and Bell nonlocality decay continuously when the temperature is increased. This decay is mainly due to the thermal relaxation effects. As the temperature reaches relatively higher value, the quantum steering and Bell nonlocality eventually reaches zero. It should be stressed that Bell nonlocality is much higher in general than quantum steering in the case of lower temperature. By contrast, for higher temperature, the quantum steering and Bell nonlocality are become vanish.

We remark, that the quantum steerability $\mathcal{S}_{A\to B}(\hat{\varrho})$ and $\mathcal{S}_{B\to A}(\hat{\varrho})$ are bounded by the Bell nonlocality $\mathcal{B}(\hat{\varrho})$. We observe, that quantum steering is two-way steering, i.e., $\mathcal{S}_{A\to B}>0$ and $\mathcal{S}_{B\to A}>0$ in the case of $T\leqslant 2.27$, as depicted in figure 2(c). Moreover, the quantum steering is one-way steering, reached for $2.27\leqslant T\leqslant 2.76$, i.e., $\mathcal{S}_{A\to B}>0$, $\mathcal{S}_{B\to A}=0$ (quantum dot 1 can steer quantum dot 2, while quantum dot 2 cannot steer quantum dot 1). Moreover, the quantum steering is no-way steering, reached for $T\geqslant 2.55$, i.e., $\mathcal{S}_{A\to B}=\mathcal{S}_{B\to A}=0$. Indeed, entangle state is always steerable, while the steerable state is not always entangled state.

4. Controlling EPR steering and Bell nonlocality via local filtering operation

In practice, a quantum system exposed in the environment will result in quantum decoherence or dissipation which is a huge threat for the system. Therefore, knowing how to suppress the effect from environment and restrain the dissipation of quantum correlation is significant in realistic quantum information processing and communication. In recent years, a number of researchers have proposed various methodologies to retard the damping of the state, such as local weak measurements [49, 50], local filtering operation (LFO) [51, 52] and parity-time symmetric operations [53, 54]. The filtering operation is characterized by a non-trace-preserving map (NTPM), which is known to be capable of increasing entanglement with some probability [55]. Practically, this map can be viewed as a null-result weak measurement [56]. To improve the EPR steering and Bell nonlocality of two-coupled DQDs states which are lost in the environment, we perform a local filtering operation on the quantum state. In our scheme, we assume that the user Alice only implements a local filtering operation on the qubit A of the system. The local filtering operation can be given in the computational basis $\{|1\rangle, |0\rangle\}$ as [57, 58]

$$\hat{E}=\sqrt{1-k}\,|0\rangle\langle 0|+\sqrt{k}\,|1\rangle\langle 1|, \tag{27}$$

where k is the strength of the filtering operation with $0\leqslant k\leqslant 1$.

To improve the Bell nonlocality and quantum steerability of quantum states which are lost in the environment, we perform a local filtering operation on the quantum state (6). When the operation is performed on particle A, the final state can be expressed by

$$\tilde{\varrho}_{AB}=\frac{(\hat{E}\otimes\hat{I})\,\hat{\varrho}_{AB}(\hat{E}\otimes\hat{I})^{\dagger}}{Tr[(\hat{E}\otimes\hat{I})\,\hat{\varrho}_{AB}(\hat{E}\otimes\hat{I})^{\dagger}]}. \tag{28}$$

Substituting $\hat{\varrho}_{AB}$ in equation (28) by equation (6), then we obtain an evolutionary quantum state

$$\tilde{\varrho}(T)=\begin{pmatrix}\tilde{\varrho}_{11} & \tilde{\varrho}_{12} & \tilde{\varrho}_{13} & \tilde{\varrho}_{14}\\ \tilde{\varrho}_{12} & \tilde{\varrho}_{22} & \tilde{\varrho}_{23} & \tilde{\varrho}_{13}\\ \tilde{\varrho}_{13} & \tilde{\varrho}_{23} & \tilde{\varrho}_{33} & \tilde{\varrho}_{34}\\ \tilde{\varrho}_{14} & \tilde{\varrho}_{13} & \tilde{\varrho}_{34} & \tilde{\varrho}_{44}\end{pmatrix}, \tag{29}$$

where, the corresponding entries are provided by

$$\begin{aligned}
&\tilde{\varrho}_{11}=\frac{\hat{\varrho}_{11}}{\hat{\varrho}_{11}+\hat{\varrho}_{22}}(1-k),\ \tilde{\varrho}_{12}=\frac{\hat{\varrho}_{12}}{\hat{\varrho}_{11}+\hat{\varrho}_{22}}(1-k),\\
&\tilde{\varrho}_{13}=\frac{\hat{\varrho}_{13}}{\hat{\varrho}_{11}+\hat{\varrho}_{22}}\sqrt{(1-k)k},\ \tilde{\varrho}_{14}=\frac{\hat{\varrho}_{14}}{\hat{\varrho}_{11}+\hat{\varrho}_{22}}\sqrt{(1-k)k},\\
&\tilde{\varrho}_{22}=\frac{\hat{\varrho}_{22}}{\hat{\varrho}_{11}+\hat{\varrho}_{22}}(1-k),\ \tilde{\varrho}_{23}=\frac{\hat{\varrho}_{23}}{\hat{\varrho}_{11}+\hat{\varrho}_{22}}\sqrt{(1-k)k},\\
&\tilde{\varrho}_{33}=\frac{\hat{\varrho}_{22}}{\hat{\varrho}_{11}+\hat{\varrho}_{22}}k,\ \tilde{\varrho}_{34}=\frac{\hat{\varrho}_{12}}{\hat{\varrho}_{11}+\hat{\varrho}_{22}}k,\ \tilde{\varrho}_{44}=\frac{\hat{\varrho}_{11}}{\hat{\varrho}_{11}+\hat{\varrho}_{22}}k.
\end{aligned} \tag{30}$$

We find that the evolutionary quantum state performed via filtering operation is not an centrosymmetric (CS) state coincidentally. For the mixed state equation (29), we can obtain the Bell-CHSH inequality maximum violation by the following form

$$\begin{aligned}
&\mathcal{B}_{\text{Bell}-\text{CHSH}}=2\max\{\tilde{\mathcal{B}}_1,\tilde{\mathcal{B}}_2,\tilde{\mathcal{B}}_3\},\\
&\tilde{\mathcal{B}}_1=\sqrt{\tilde{\mu}_1+\tilde{\mu}_2},\\
&\tilde{\mathcal{B}}_2=\sqrt{\tilde{\mu}_1+\tilde{\mu}_3},\\
&\tilde{\mathcal{B}}_3=\sqrt{\tilde{\mu}_2+\tilde{\mu}_3},
\end{aligned} \tag{31}$$

where

$$\begin{aligned}
&\tilde{\mu}_1=4(\tilde{\varrho}_{14}-\tilde{\varrho}_{23})^2,\\
&\tilde{\mu}_2=\frac{1}{2}\left(\begin{array}{l}4\tilde{\varrho}_{\alpha}^2+4\tilde{\varrho}_{\beta}^2+\tilde{\varrho}_{\gamma}^2\\ +\sqrt{16(\tilde{\varrho}_{\alpha}^2+\tilde{\varrho}_{\beta}^2)^2+8(-\tilde{\varrho}_{\alpha}^2+\tilde{\varrho}_{\beta}^2)\tilde{\varrho}_{\gamma}^2+\tilde{\varrho}_{\gamma}^4}\end{array}\right),\\
&\tilde{\mu}_3=\frac{1}{2}\left(\begin{array}{l}4\tilde{\varrho}_{\alpha}^2+4\tilde{\varrho}_{\beta}^2+\tilde{\varrho}_{\gamma}^2\\ -\sqrt{16(\tilde{\varrho}_{\alpha}^2+\tilde{\varrho}_{\beta}^2)^2+8(-\tilde{\varrho}_{\alpha}^2+\tilde{\varrho}_{\beta}^2)\tilde{\varrho}_{\gamma}^2+\tilde{\varrho}_{\gamma}^4}\end{array}\right),
\end{aligned} \tag{32}$$

and

$$\begin{aligned}
\tilde{\varrho}_{\alpha}&=\tilde{\varrho}_{14}+\tilde{\varrho}_{23},\\
\tilde{\varrho}_{\beta}&=\tilde{\varrho}_{12}-\tilde{\varrho}_{34},\\
\tilde{\varrho}_{\gamma}&=\tilde{\varrho}_{11}-\tilde{\varrho}_{22}-\tilde{\varrho}_{33}+\tilde{\varrho}_{44}.
\end{aligned} \tag{33}$$

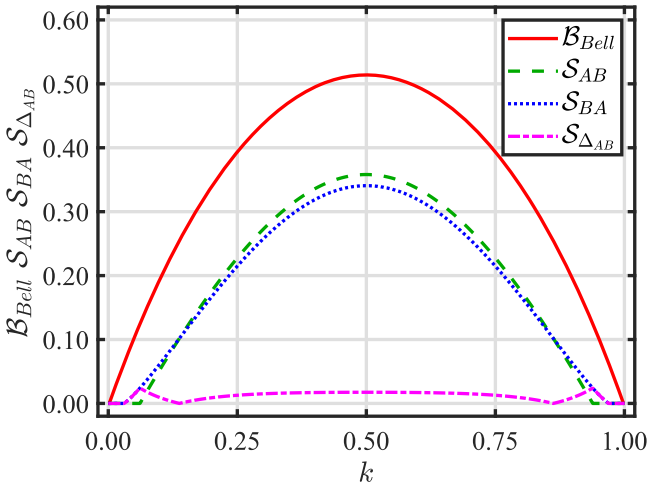

Figure 3. The variation (evolution) of Bell nonlocality and quantum steerability as a function of the filtering parameter k with $T = 1.0$, $V = 20\ \mu eV$, $\Delta_1 = 10\ \mu eV$ and $\Delta_2 = 3\ \mu eV$. The fixed parameter is $k_B = 1$.

By using Pauli matrices ($\hat{\sigma}_x$, $\hat{\sigma}_y$, $\hat{\sigma}_z$) measurements, one can simplify the expression of EPR steering inequality in equation (11) reads,

$$\tilde{\mathcal{I}}_{ab} = \frac{1}{2}\sum_{i=1}^{4}\begin{bmatrix}(\tilde{P}^{ab}_{x_i})\log_2(\tilde{P}^{ab}_{x_i})\\ +(\tilde{P}^{ab}_{y_i})\log_2(\tilde{P}^{ab}_{y_i})\\ +(\tilde{P}^{ab}_{z_i})\log_2(\tilde{P}^{ab}_{z_i})\end{bmatrix} - \sum_{i=1}^{2}\begin{bmatrix}(\tilde{P}^{a}_{x_i})\log_2(\tilde{P}^{a}_{x_i})\\ +(\tilde{P}^{a}_{y_i})\log_2(\tilde{P}^{a}_{y_i})\\ +(\tilde{P}^{a}_{z_i})\log_2(\tilde{P}^{a}_{z_i})\end{bmatrix}, \tag{34}$$

where $\tilde{P}^{ab}_{x_i}$, $\tilde{P}^{ab}_{y_i}$ and $\tilde{P}^{ab}_{z_i}$ represent the eigenvalues of the density operator $\tilde{\varrho}(T)$. Explicitly,

they are given by

$$\begin{aligned}\tilde{P}^{ab}_{x_1} &= 1 + 2(\tilde{\varrho}_{13} + 2\tilde{\varrho}_{14} + \tilde{\varrho}_{24}),\\ \tilde{P}^{ab}_{x_2} &= 1 - 2(\tilde{\varrho}_{13} - 2\tilde{\varrho}_{14} + \tilde{\varrho}_{24}),\\ \tilde{P}^{ab}_{x_3} &= 1 - 2(-\tilde{\varrho}_{13} + 2\tilde{\varrho}_{14} - \tilde{\varrho}_{24}),\\ \tilde{P}^{ab}_{x_4} &= 1 + 2(-\tilde{\varrho}_{13} - 2\tilde{\varrho}_{14} - \tilde{\varrho}_{24}),\\ \tilde{P}^{ab}_{y_1,y_2,y_3,y_4} &= 1,\\ \tilde{P}^{ab}_{z_i} &= 4\tilde{\varrho}_{ii}.\end{aligned} \tag{35}$$

Likewise, $\tilde{P}^{a}_{x_i}$, $\tilde{P}^{a}_{y_i}$ and $\tilde{P}^{a}_{z_i}$ are the eigenvalues of the reduced density operator $\hat{\varrho}_A$, where,

$$\begin{aligned}\tilde{P}^{a}_{x_1,x_2} &= 1 \pm 2(\tilde{\varrho}_{13} + \tilde{\varrho}_{24}),\ \tilde{P}^{a}_{y_1,y_2} = 1,\\ \tilde{P}^{a}_{z_1,z_2} &= 1 \pm (\tilde{\varrho}_{11} + \tilde{\varrho}_{22} - \tilde{\varrho}_{33} - \tilde{\varrho}_{44}).\end{aligned} \tag{36}$$

The degree of steerability is quantified based on Alice's measurements as follows

$$\mathcal{S}_{A\to B} = \max\left\{0, \frac{\tilde{\mathcal{I}}_{ab} - 2}{\tilde{\mathcal{I}}_{\max} - 2}\right\}, \tag{37}$$

where $\tilde{\mathcal{I}}_{\max} = 6$ is calculated for a system initially prepared in Bell states. The factor $(\tilde{\mathcal{I}}_{\max} - 2)$ is introduced to ensure that the steering process is normalized. By exchanging the roles of A and B, the possibility of the steering by performing measurements on the subsystem B is given by,

$$\mathcal{S}_{B\to A} = \max\left\{0, \frac{\tilde{\mathcal{I}}_{ba} - 2}{\tilde{\mathcal{I}}_{\max} - 2}\right\}, \tag{38}$$

where $\tilde{\mathcal{I}}_{ba}$ quantifies the steering from Bob to Alice, it is given by,

$$\tilde{\mathcal{I}}_{ba} = \frac{1}{2}\sum_{i=1}^{4}\begin{bmatrix}(\tilde{P}^{ab}_{x_i})\log_2(\tilde{P}^{ab}_{x_i})\\ +(\tilde{P}^{ab}_{y_i})\log_2(\tilde{P}^{ab}_{y_i})\\ +(\tilde{P}^{ab}_{z_i})\log_2(\tilde{P}^{ab}_{z_i})\end{bmatrix} - \sum_{i=1}^{2}\begin{bmatrix}(\tilde{P}^{b}_{x_i})\log_2(\tilde{P}^{b}_{x_i})\\ +(\tilde{P}^{b}_{y_i})\log_2(\tilde{P}^{b}_{y_i})\\ +(\tilde{P}^{b}_{z_i})\log_2(\tilde{P}^{b}_{z_i})\end{bmatrix}, \tag{39}$$

with

$$\begin{aligned}\tilde{P}^{b}_{x_1,x_2} &= 1 \pm 2(\tilde{\varrho}_{13} + \tilde{\varrho}_{24}),\ \tilde{P}^{b}_{y_1,y_2} = 1,\\ \tilde{P}^{b}_{z_1,z_2} &= 1 \pm (\tilde{\varrho}_{11} - \tilde{\varrho}_{22} + \tilde{\varrho}_{33} - \tilde{\varrho}_{44}).\end{aligned} \tag{40}$$

Figure 3 illustrates the Bell nonlocality and quantum steerability as a function of the filtering parameter k. The results of Bell nonlocality $\mathcal{B}_{Bell}$ (red solid line), quantum steerability $\mathcal{S}_{A\to B}$ (green dash line), $\mathcal{S}_{B\to A}$ (blue dot-dash line) and the steering difference $\mathcal{S}_{\Delta_{AB}}$ (purple dot line) between $\mathcal{S}_{A\to B}$ and $\mathcal{S}_{B\to A}$ are displayed in turn. The Bell nonlocality $\mathcal{B}_{Bell}$ and steerability $\mathcal{S}_{A\to B}$, $\mathcal{S}_{B\to A}$, as well as steerability asymmetry $\mathcal{S}_{\Delta_{AB}}$ show a symmetric behavior with respect to the filtering parameter k. The Bell nonlocality and EPR steering initially increases and then gradually decreases with the increase of the filtering parameter k. Notably, the optimal Bell nonlocality and EPR steering occurs when the filtering parameter $k = 0.5$. When the filtering parameter k fulfills $0.0615 \leqslant k \leqslant 0.9387 (0.0308 \leqslant k \leqslant 0.9694)$, the quantum steerability $\mathcal{S}_{A\to B}(\mathcal{S}_{B\to A})$ is symmetrical. One can easily find that the filtering parameter k will induce asymmetry steering. Obviously, steering $\mathcal{S}_{A\to B}$ is not equal to the steering $\mathcal{S}_{B\to A}$ for most parameters $0.0308 \leqslant k \leqslant 0.9694$, except for the points $k = 0.1378, 0.8624$. Interestingly, we find that steering $\mathcal{S}_{A\to B}$ is always larger than $\mathcal{S}_{B\to A}$ for almost all $0.1378 \leqslant k \leqslant 0.8624$ and that steering $\mathcal{S}_{A\to B}$ is always lower than $\mathcal{S}_{B\to A}$ for almost all $0.0308 \leqslant k \leqslant 0.1378$ or $0.8624 \leqslant k \leqslant 0.9694$. When $0.0615 \leqslant k \leqslant 0.9387$, the steering is asymmetrical and a steering difference appears

$\mathcal{S}_{\Delta_{AB}} \geqslant 0$ (two way). Two-way quantum steering is a significant and consequential resource for secure quantum teleportation of the two-coupled DQDs system. In addition, $\mathcal{S}_{A\to B}$ increases (or decreases) faster than $\mathcal{S}_{B\to A}$. When $0.0308 \leqslant k \leqslant 0.0615$ or $0.9387 \leqslant k \leqslant 0.9694$, one always has $\mathcal{S}_{B\to A} > 0$, $\mathcal{S}_{A\to B} = 0$ and the steering difference then becomes $\mathcal{S}_{\Delta_{AB}} = \mathcal{S}_{B\to A} > 0$ (one way). When $k \leqslant 0.0308$ or $k \geqslant 0.9694$, the steering is zero and $\mathcal{S}_{A\to B} = \mathcal{S}_{B\to A} = \mathcal{S}_{\Delta_{AB}}$ (no way). When $k = 0$ or $k = 1$, $\mathcal{S}_{\Delta AB} = \mathcal{S}_{A\to B} = \mathcal{S}_{B\to A} = 0$, it means no perfect communication. It is obvious that Bell nonlocality and quantum steerability will be reduced in the filtering parameter region, $0.5 < k < 1$ (or upgraded in the filtering parameter region, $0 < k < 0.5$) when the strength of filtering operation is strengthened.

In practice, filtering operations can regulate the exchange of information between qubits and the environment. In the two-coupled DQDs' system composed of two excess electrons (qubits) and a hierarchical environment, the quantum state is affected by the parameter k. That is to say, the filtering operation of qubit A will lead to the change of information flow. Moreover, to check the degree of asymmetry of steerability under the filtering parameter, we define EPR steering asymmetry as $\mathcal{S}_{\Delta_{AB}}$. Then, we show the Bell nonlocality $\mathcal{B}_{\rm Bell}$ and steerability $\mathcal{S}_{A\to B}$, $\mathcal{S}_{B\to A}$, as well as steerability asymmetry $\mathcal{S}_{\Delta_{AB}}$ as a function of the Coulomb potential V, tunneling parameters Δ_1 and environment temperature T for fixed filtering parameter k in figures 4–6. The evolution of $\mathcal{B}_{\rm Bell}$ as well as $\mathcal{S}_{A\to B}$ and $\mathcal{S}_{B\to A}$ are plotted for three values of channel correlation strength: no operation (red lines), $k = 0.2$(blue lines) and $k = 0.3$ (green lines).

In figure 4, we plot the Bell nonlocality and quantum steerability as a function of the Coulomb potential V with $T = 1.0$, $\Delta_1 = 10\,\mu$eV, $\Delta_2 = 3\,\mu$eV and $k_{\rm B} = 1$, for different values of the parameter $k = 0.20, 0.30$. The red line is plotted with no operation, the blue line with $k = 0.2$ and the green line with $k = 0.3$ It can be observed from figure 4 that after performing the filtering operation, the amplitude of Bell nonlocality and quantum steerability is improved as the Coulomb potential V increases by in the filtering parameter region, $0 < k < 0.5$. Hence, we can make use of the appropriate filtering operation to extend the available range of variate Coulomb potential V. Figure 4 shows that the Bell nonlocality and quantum steerability are absent when the Coulomb potential V is zero. This result shows that the Coulomb potential V can be used for either turning on or off the Bell nonlocality and quantum steerability. It becomes clear that the Coulomb interaction between the two excess electrons have to be adjusted to a specific interval to utilize quantum correlations for better resourcefulness in the two-coupled DQDs system.

In figure 5, we plot the Bell nonlocality and quantum steerability as a function of the tunneling parameters Δ_1 with $T = 1.0$, $V = 20\,\mu$eV, $\Delta_2 = 3\,\mu$eV and $k_{\rm B} = 1$, for different values of the parameter $k = 0.20, 0.30$. Now let us consider the effect of the tunneling parameters Δ_1. We can observe that the Bell nonlocality and quantum steerability vanish when $\Delta_1 = 0$ regardless of the values of Δ_2 in figure 5. In this case, the two-coupled DQDs are not entangled, because the

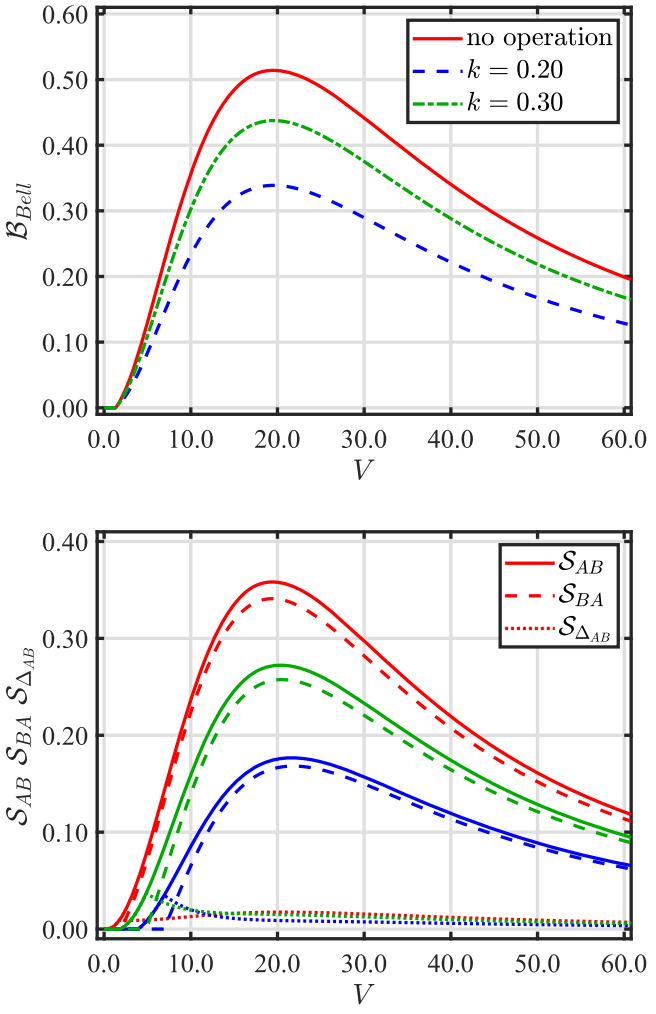

Figure 4. Bell nonlocality and quantum steerability as a function of the Coulomb potential V with $T = 1.0$, $\Delta_1 = 10\,\mu eV$, $\Delta_2 = 3\,\mu eV$ and $k_B = 1$, for different values of the filtering parameter $k = 0.20, 0.30$. The red line is plotted with no operation, the blue line with $k = 0.2$ and the green line with $k = 0.3$. Graph (a) shows the Bell nonlocality. Graph (b) shows the quantum steerability $\mathcal{S}_{A\to B}$ (solid line) and $\mathcal{S}_{B\to A}$ (dash line), and asymmetry $\mathcal{S}_{\Delta_{AB}}$ (dot line) between Alice and Bob.

electron can no longer move within the double quantum dots. The range of Bell nonlocality and quantum steerability can be prolonged when the filtering parameter $k = 0.30$.

We can improve the value of the Bell nonlocality and quantum steerability sometimes in some certain range of tunneling parameters Δ_1. However, as one switches on the filtering process, the steering inequality is not satisfied at larger values of the tunneling parameters Δ_1. In this situation, the decoherence arises and consequently the degree of quantum steerability decreases as the tunneling parameters Δ_1 increases. It is worth mentioning that the filtering process does not increase the degree of steerability, but decreases the range of quantum steerability. This phenomenon is displayed by comparing figure 5(b), where the steerable areas are enlarged as the filtering parameter increases until $k = 0.5$.

In addition, it is worth noting that there is an unusual phenomenon, we take $k = 0.30$, at the left-hand of the

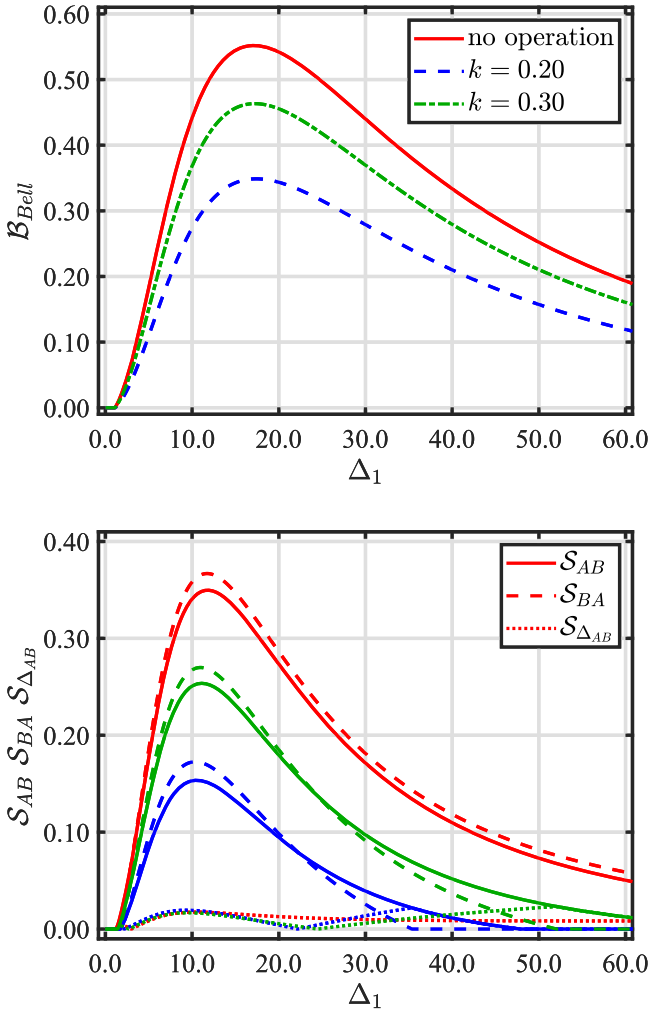

Figure 5. Bell nonlocality and quantum steerability as a function of the tunneling parameters Δ_1 with $T = 1.0$, $V = 20\ \mu eV$, $\Delta_2 = 3\ \mu eV$ and $k_B = 1$, for different values of the filtering parameter $k = 0.20, 0.30$. The red line is plotted with no operation, the blue line with $k = 0.2$ and the green line with $k = 0.3$. Graph (a) shows the Bell nonlocality. Graph (b) shows the quantum steerability $\mathcal{S}_{A\to B}$ (solid line) and $\mathcal{S}_{B\to A}$ (dash line), and asymmetry $\mathcal{S}_{\Delta_{AB}}$ (dot line) between Alice and Bob.

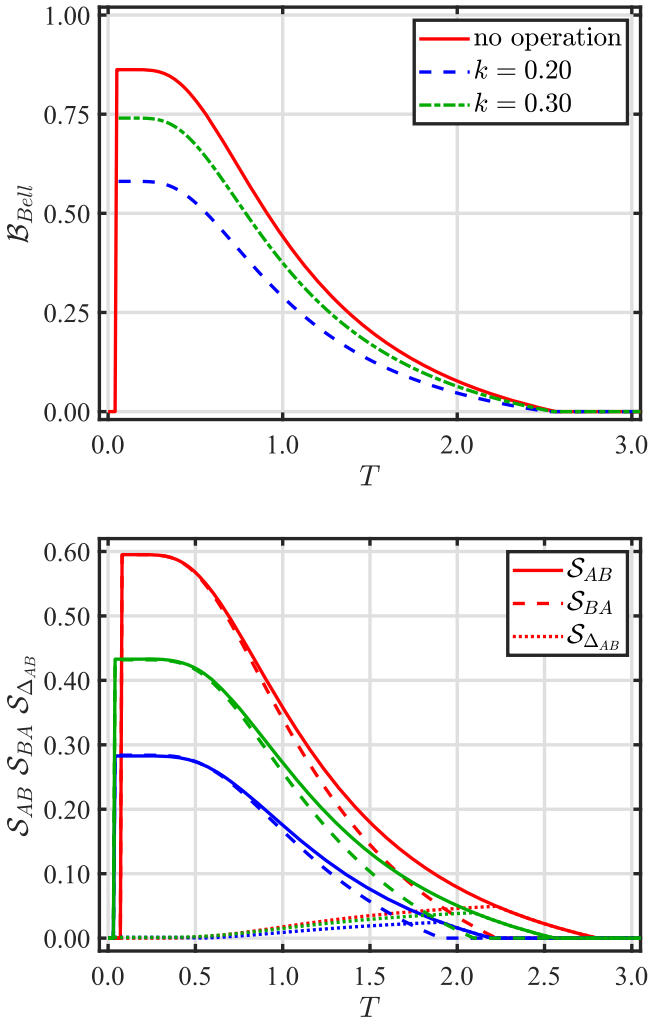

Figure 6. Bell nonlocality and quantum steerability as a function of the temperature T with $V = 20\ \mu eV$, $\Delta_1 = 10\ \mu eV$, $\Delta_2 = 3\ \mu eV$ and $k_B = 1$, for different values of the filtering parameter $k = 0.20, 0.30$. The red line is plotted with no operation, the blue line with $k = 0.2$ and the green line with $k = 0.3$ Graph (a) shows the Bell nonlocality. Graph (b) shows the quantum steerability $\mathcal{S}_{A\to B}$ (solid line) and $\mathcal{S}_{B\to A}$ (dash line), and asymmetry $\mathcal{S}_{\Delta_{AB}}$ (dot line) between Alice and Bob.

threshold value $\Delta_{1C} = 24.691\,\mu\text{eV}$ in figure 5(b), EPR steering $\mathcal{S}_{A\to B}$ (green solid line) is lower than $\mathcal{S}_{B\to A}$ (green dash line) between Alice and Bob. On the contrary, the right hand of the threshold value $\Delta_{1C} = 24.691\,\mu\text{eV}$, EPR steering $\mathcal{S}_{A\to B}$ (green solid line) is higher than $\mathcal{S}_{B\to A}$ (green dash line) between Alice and Bob. The EPR steering asymmetry $\mathcal{S}_{\Delta_{AB}}$ (green dot line) between Alice and Bob first increase, then decrease to zero and finally increase as the tunneling strength Δ_1 increases. However, this phenomenon does not appear with no operation between Alice and Bob.

In figure 6, we plot the Bell nonlocality and quantum steerability as a function of the temperature with $V = 20\,\mu\text{eV}$, $\Delta_1 = 10\,\mu\text{eV}$, $\Delta_2 = 3\,\mu\text{eV}$ and $k_\text{B} = 1$, for different values of the parameter k. It is easy to see that the Bell nonlocality and quantum steerability in the two-coupled DQDs system with no filtering operation undergoes a rapid decrease when the temperature T increases. It also can be seen that for a given value of the parameter k, the Bell nonlocality and quantum steerability is destroyed when the parameter k decreases in the filtering parameter region $0 < k < 0.5$. The Bell nonlocality and quantum steerability $\mathcal{S}_{A\to B}$ and $\mathcal{S}_{B\to A}$ are monotonically decreasing functions of the temperature T until a threshold value T_C, which means that decoherence can cause the degradation of EPR steering. These findings allow us to conclude that the filtering operation in the system induces the loss of quantum correlations. Figure 5 shows that both the Bell nonlocality and quantum steerability decay continuously when the temperature is increased. This decay is mainly due to the thermal relaxation effects. As the temperature reaches relatively higher values, the Bell nonlocality and quantum steerability vanish, though the former is more resistant than the latter as it relatively survives more. It should be stressed that Bell nonlocality are in general much higher than quantum steerability in the case of lower temperature. By

contrast in figure 6, the Bell nonlocality and quantum steerability will be disappeared in zero temperature. Figure 6(b) investigates how variations of the temperature T influences the direction of quantum steerability by examining $\mathcal{S}_{A\to B}$ and $\mathcal{S}_{B\to A}$. We demonstrate the symmetric EPR steering as a function of the environment temperature T with varying filtering parameter $k = 0.2, 0.3$. It can be observed that the larger filtering parameter $k = 0.3$ $(0 < k < 0.5)$ can lead to stronger robustness against temperature for the EPR steering. Under the effect of the filtering parameter k, the quantum steerability $\mathcal{S}_{B\to A}$ can survive up to the temperature of $T = 1.910(2.100)$ when $k = 0.20(0.30)$. As is evident from the plot, it is possible to achieve quantum steerability asymmetry $\mathcal{S}_{\Delta_{AB}}$ under different temperatures. Furthermore, the one-way EPR steering can be achieved within a specific temperature range (approximately $T = 2.100$ to $T = 2.560$) under the effect of the filtering parameter $k = 0.30$, which provides an effective mean for manipulating the one-way EPR steering by adjusting the temperature. It clearly shows that the maximum value steerability asymmetry for one-way steering appears with no operation. Apparently, the one-way steering evolves with the filtering parameter k maximized at $k = 0.5$.

As can been seen from figures 2–6, the peaks of Bell nonlocality and quantum steerability do not coincide completely. The reason is that quantum correlations are not equivalent in general. This is due to the fact that different measures of quantum states lack the same ordering. Additionally, the sudden change points of Bell nonlocality emerge earlier compared to quantum steerability. We should emphasize that the value of Bell nonlocality and quantum steerability are confined in the following inequality

$$0 \leqslant \mathcal{S}(\hat{\varrho}) \leqslant \mathcal{B}(\hat{\varrho}) \leqslant 1, \tag{41}$$

where the upper bound 1 indicates the maximum quantum correlation.

5. Conclusions

In the present work, we have studied the dynamics of quantum steering and Bell nonlocality of two-coupled DQDs with two excess electrons. In the model, Bell nonlocality and quantum steerability is solved exactly with and without the local filtering operation. The influence of the finite temperature, the weight of the Coulomb coupling between electrons and tunneling coupling between the charge qubits on Bell nonlocality and quantum steerability are investigated. We find that the filtering process does not increase the degree of steerability, but decreases the range of quantum steerability. In addition, we should emphasize that Bell nonlocality is always greater than quantum steerability. Furthermore, we reveal an intrinsic feature that the quantifier of the quantum discord and geometric quantum discord exhibit a dynamical behavior to be different from each other by showing that it actually coincides with a simpler quantity based on von Neumann measurements. More importantly, the EPR steering asymmetry between Alice and Bob first increase, then decrease to zero and finally increase as tunneling strength increases. However, this unusual phenomenon does not appear with no operation between Alice and Bob. It is expected that EPR steering can be seen as a better resource for implementing quantum information processing in the two-coupled DQDs system.

Acknowledgments

This work is supported by the University-Industry Collaborative Education Program (Project No. 220506627183928).

Conflict of interest

The authors declare no conflict of interest.

References

[1] Peled B Y, Te'eni A, Carmi A and Cohen E 2021 Correlation minor norms, entanglement detection and discord *Sci. Rep.* **11** 2849
[2] Wootters W K 1998 Entanglement of formation of an arbitrary state of two qubits *Phys. Rev. Lett.* **80** 2245
[3] Schrödinger E 1935 Discussion of probability relations between separated systems *Math. Proc. Cambridge Philos. Soc.* **31** 555
[4] Bell J S 1964 On the Einstein–Podolsky rosen paradox *Phys. Phys. Fizika* **1** 195
[5] Ollivier H and Zurek W H 2001 Quantum discord: a measure of the quantumness of correlations *Phys. Rev. Lett.* **88** 017901
[6] Horodecki R, Horodecki P, Horodecki M and Horodecki K 2009 Quantum entanglement *Rev. Mod. Phys.* **81** 865
[7] Wiseman H M, Jones S J and Doherty A C 2007 Steering, entanglement, nonlocality, and the Einstein–Podolsky–Rosen paradox *Phys. Rev. Lett.* **98** 140402
[8] Jones S J, Wiseman H M and Doherty A C 2007 Entanglement, Einstein–Podolsky–Rosen correlations, Bell nonlocality, and steering *Phys. Rev.* A **76** 052116
[9] Walborn S P, Salles A, Gomes R M, Toscano F and Souto Ribeiro P H 2011 Revealing hidden Einstein–Podolsky–Rosen nonlocality *Phys. Rev. Lett.* **106** 130402
[10] Schneeloch J, Broadbent C J, Walborn S P, Cavalcanti E G and Howell J C 2013 Einstein–Podolsky–Rosen steering inequalities from entropic uncertainty relations *Phys. Rev.* A **87** 062103
[11] Skrzypczyk P, Navascués M and Cavalcanti D 2014 Quantifying Einstein–Podolsky–Rosen steering *Phys. Rev. Lett.* **112** 180404
[12] Händchen V, Eberle T, Steinlechner S, Samblowski A, Franz T, Werner R F and Schnabel R 2012 Observation of one-way Einstein–Podolsky–Rosen steering *Nat. Photon.* **6** 596
[13] Uola R, Costa A C S, Nguyen H C and Gühne O 2020 Quantum steering *Rev. Mod. Phys.* **92** 015001
[14] Zhao Y Y, Ku H Y, Chen S L, Chen H B, Nori F, Xiang G Y, Li C F, Guo G C and Chen Y N 2020 Experimental demonstration of measurement-device-independent measure of quantum steering *npj. Quantum Inf.* **6** 77
[15] Tavakoli A 2024 Quantum steering with imprecise measurements *Phys. Rev. Lett.* **132** 070204

[16] Scarani V, Bechmann-Pasquinucci H, Cerf N J, Dušek M, Lütkenhaus N and Peev M 2009 The security of practical quantum key distribution *Rev. Mod. Phys.* **81** 1301

[17] Cavalcanti D, Skrzypczyk P, Aguilar G, Nery R, Ribeiro P S and Walborn S 2015 Detection of entanglement in asymmetric quantum networks and multipartite quantum steering *Nat. Commun.* **6** 1–6

[18] Skrzypczyk P and Cavalcanti D 2018 Maximal randomness generation from steering inequality violations using qudits *Phys. Rev. Lett.* **120** 260401

[19] Guo Y, Cheng S, Hu X, Liu B H, Huang E M, Huang Y F, Li C F, Guo G C and Cavalcanti E G 2019 Experimental measurement-device-independent quantum steering and randomness generation beyond qubits *Phys. Rev. Lett.* **123** 170402

[20] Curchod F J, Johansson M, Augusiak R, Hoban M J, Wittek P and Acìn A 2017 Unbounded randomness certification using sequences of measurements *Phys. Rev.* A **95** 020102

[21] Bell J S 1966 On the problem of hidden variables in quantum mechanics *Rev. Mod. Phys.* **38** 447–52

[22] Clauser J F, Horne M A, Shimony A and Holt R A 1969 Proposed experiment to test local hidden-variable theories *Phys. Rev. Lett.* **23** 880

[23] Bartkiewicz K, Horst B, Lemr K and Miranowicz A 2013 Entanglement estimation from Bell inequality violation *Phys. Rev.* A **88** 052105

[24] Giustina M *et al* 2015 Significant-loophole-free test of Bell's theorem with entangled photons *Phys. Rev. Lett.* **115** 250401

[25] Storz S *et al* 2023 Loophole-free Bell inequality violation with superconducting circuits *Nature* **617** 265–70

[26] Nadlinger D P *et al* 2022 Experimental quantum key distribution certified by Bell's theorem *Nature* **607** 682–6

[27] Wooltorton L, Brown P and Colbeck R 2024 Device-independent quantum key distribution with arbitrarily small nonlocality *Phys. Rev. Lett.* **132** 210802

[28] Mohamed A-B A, Rahman A and Aldosari F 2023 Thermal quantum memory, Bell-non-locality, and entanglement behaviors in a two-spin Heisenberg chain model *Alex. Eng. J.* **66** 861–71

[29] Nath P P, Saha D, Home D and Sinha U 2024 Single-system-based generation of certified randomness using leggett-garg inequality *Phys. Rev. Lett.* **133** 020802

[30] Einstein A, Podolsky B and Rosen N 1935 Can quantum-mechanical description of physical reality be considered complete? *Phys. Rev.* **47** 777

[31] Genovese M 2005 Research on hidden variable theories: a review of recent progresses *Phys. Rep.* **413** 319

[32] Brunner N, Cavalcanti D, Pironio S, Scarani V and Wehner S 2014 Bell nonlocality *Rev. Mod. Phys.* **86** 419

[33] Fanchini F F, Castelano L K and Caldeira A O 2010 Entanglement versus quantum discord in two coupled double quantum dots *New J. Phys.* **12** 073009

[34] Filgueiras C, Rojas O and Rojas M 2020 Thermal entanglement and correlated coherence in two coupled double quantum dots systems *Ann. Phys.* **532** 2000207

[35] Mansour H A, Faqir M and Baz M E 2023 Global quantum discord and entanglement in two coupled double quantum dots AlGaAs/GaAs *Int. J. Theor. Phys.* **62** 58

[36] Mohammed N I, Abdelsalam H M, Almalki S, Abd-Rabbou M Y, Abdel-Khalek S and Khalil E M 2023 Witnessing quantum correlations in two coupled quantum dots under intrinsic decoherence *Alex. Eng. J.* **69** 521

[37] Ait Chlih A, Rahman A and Habiballah N 2024 Prospecting quantum correlations and examining teleportation fidelity in a pair of coupled double quantum dots system *Ann. Phys.* **536** 2300434

[38] Hosseiny S M 2024 Quantum dense coding and teleportation based on two coupled quantum dot molecules influenced by intrinsic decoherence, tunneling rates, and Coulomb coupling interaction *Appl. Phys.* B **130** 8

[39] de Oliveira J L D, Rojas M and Filgueiras C 2021 Two coupled double quantum-dot systems as a working substance for heat machines *Phys. Rev.* E **104** 014149

[40] Elghaayda S, Dahbi Z and Mansour M 2022 Local quantum uncertainty and local quantum Fisher information in two-coupled double quantum dots *Opt. Quant. Electron* **54** 419

[41] Mirzaei S 2022 The effect of intrinsic decoherence on quantum dynamics of two coupled double quantum dot systems *Physica* B **644** 414175

[42] Andrew A L 1998 Classroom note: centrosymmetric matrices *SIAM Rev* **40** 697

[43] Schneeloch J, Broadbent C J, Walborn S P, Cavalcanti E G and Howell J C 2013 Einstein–Podolsky–Rosen steering inequalities from entropic uncertainty relations *Phys. Rev.* A **87** 062103

[44] Sun W Y, Wang D, Shi J D and Ye L 2017 Exploration quantum steering, nonlocality and entanglement of two-qubit X-state in structured reservoirs *Sci. Rep.* **7** 39651

[45] Abd-Rabbou M Y, Metwally N, Ahmed M M A and Obada A S F 2022 Improving the bidirectional steerability between two accelerated partners via filtering process *Mod. Phys. Lett.* A **20** 2250143

[46] Verstraete F and Wolf M M 2002 Entanglement versus Bell violations and their behavior under local filtering operations *Phys. Rev. Lett.* **89** 170401

[47] Horodecki R, Horodecki P and Horodecki M 1995 Violating Bell inequality by mixed spin-1/2 states: necessary and sufficient condition *Phys. Lett.* A **200** 340

[48] Bartkiewicz K, Lemr K, Cernoch A and Miranowicz A 2017 Bell nonlocality and fully entangled fraction measured in an entanglement-swapping device without quantum state tomography *Phys. Rev.* A **95** 030102

[49] Wang S C, Yu Z W, Zou W J and Wang X B 2014 Protecting quantum states from decoherence of finite temperature using weak measurement *Phys. Rev.* A **89** 022318

[50] Kim Y S, Lee J C, Kwon O and Kim Y H 2012 Protecting entanglement from decoherence using weak measurement and quantum measurement reversal *Nature Phys.* **8** 117–20

[51] Siomau M and Kamli A A 2012 Steering quantum-memory-assisted entropic uncertainty under unital and nonunital noises via filtering operations *Phys. Rev.* A **86** 032304

[52] Abd-Rabbou M Y, Metwally N, Ahmed M M A and Obada A S F 2022 Improving the bidirectional steerability between two accelerated partners via filtering process *Mod. Phys. Lett.* A **37** 2250143

[53] Zhang S Y, Fang M F, Zhang Y L, Guo Y N, Zhao Y J and Tang W W 2015 Reduction of entropic uncertainty in entangled qubits system by local PT-symmetric operation *Chin. Phys.* B **24** 090304

[54] Dogra S, Melnikov A A and Paraoanu G S 2021 Quantum simulation of parity–time symmetry breaking with a superconducting quantum processor *Commun Phys.* **4** 26

[55] Gisin N 1996 Hidden quantum nonlocality revealed by local filters *Phys. Lett.* A **210** 151156

[56] Sun Q, Al-Amri M, Davidovich L and Zubairy M S 2010 Reversing entanglement change by a weak measurement *Phys. Rev.* A **82** 052323

[57] Huang A J, Shi J D, Wang D and Ye L 2017 Steering quantum-memory-assisted entropic uncertainty under unital and nonunital noises via filtering operations *Quantum Inf. Process* **16** 46

[58] Yang H and Xing L L 2020 Exploring the nonlocal advantage of quantum coherence and Bell nonlocality in the Heisenberg XYZ chain *Laser Phys. Lett.* **17** 095202